

Received October 9, 2016, accepted November 9, 2016, date of publication November 18, 2016,
date of current version December 8, 2016.

Digital Object Identifier 10.1109/ACCESS.2016.2630708

A DSRC-Based Vehicular Positioning Enhancement Using a Distributed Multiple-Model Kalman Filter

YUNPENG WANG¹, XUTING DUAN¹, (Student Member, IEEE),
DAXIN TIAN¹, (Senior Member, IEEE), MIN CHEN², (Senior Member, IEEE),
AND XUEJUN ZHANG³

¹Beijing Advanced Innovation Center for Big Data and Brain Computing, School of Transportation Science and Engineering, Beihang University, Beijing 100191, China

²School of Computer Science and Technology, Huazhong University of Science and Technology, Wuhan 430074, China

³School of Electronic and Information Engineering, Beihang University, Beijing 100191, China

Corresponding author: D. Tian (dtian@buaa.edu.cn)

This work was supported by the National Natural Science Foundation of China under Grant U1564212 and Grant 61672082.

ABSTRACT Some inherent shortcomings of the global positioning systems (GPSs), such as limited accuracy and availability, limit the positioning performance of a vehicular location system in urban harsh environments. This motivates the development of cooperative positioning (CP) methods based on emerging vehicle-to-anything communications. In this paper, we present a framework of vehicular positioning enhancement based on dedicated short range communications (DSRC). An interactive multiple model is first used to track the distributed manners of both the vehicle acceleration variations and the switching of the covariances of DSRC physical measurements such as the Doppler frequency shift and the received signal strength indicator, with which a novel CP enhancement method is presented to improve the distributed estimation performance by sharing the motion states and the physical measurements among local vehicles through vehicular DSRC. We have also presented an analysis on the positioning performance, and a closed-formed lower bound, named the modified square position error bound (mSPEB), is derived for bounding the positioning estimation performance of CP systems. Simulation results have been supplemented to compare our proposed method with the stand-alone GPS implementation in terms of the root-mean-square error (RMSE), showing that the obtained positioning enhancement can improve comprehensive positioning performance by the percentage varying between about 35% and about 72% under different traffic intensities and the connected vehicle penetrations. More importantly, the RMSE achieved by our method is shown remarkably closed to the root of the theoretical mSPEB.

INDEX TERMS Vehicle localization systems, vehicular positioning enhancements, dedicated short-range communications (DSRC), cooperative positioning (CP).

I. INTRODUCTION

The availability of high-accuracy location-awareness is essential for a diverse set of vehicular applications including intelligent transportation systems, location-based services (LBS), navigation, as well as a couple of emerging cooperative vehicle-infrastructure systems (CVIS) [1]. Typically, as an important technique, the real-time vehicle positioning system has drawn great attention in the fields of transportation and mobile communications [2]. However, it still faces a big challenge in the areas with inconsistent availability of satellite networks, especially in dense urban

areas where the stand-alone global navigation satellite systems (GNSSs) (e.g., GPS) cannot work well. Even though a set of high precision location equipment (e.g., DGPS) is deployed, the positioning performance is adversely impacted in non-line-of-sight (NLOS) (e.g., buildings, walls, trees, vehicles, and more obstructions) scenarios, or by the severe multi-path effect in urban canyon environments [3].

In vehicle ad-hoc networks (VANETs), it is expected that any vehicle with wireless communication capability will be able to accurately sense each other and to contribute to vehicular collision avoidance, lane departure warning,

and intersection safety enhancements [4]–[6]. Apart from the GPS, a lot of emerging location systems relying on the spatial radio frequency, such as wireless communication signals (e.g., WiFi, Cellular, RFID) or inertial navigation system (INS), are implemented [7]–[10]. In [2] and [11]–[15], the fundamental techniques in positioning systems have been presented based on the real-time measurements of time of arrival (TOA), time difference of arrival (TDOA), direction of arrival (DOA), received signal strength indicator (RSSI), Doppler frequency shift (DFS), fingerprinting, and wireless channel state information (CSI) techniques. Especially, cloud-based wireless network proposed in [16] is expected to provide flexible virtualized network functions for vehicular positioning. Recent researches indicate that these measurements are challenged by some drawbacks varying from complexities of the time-synchronization, occupations of the high-bandwidth, to huge costs on the implementations [3]. Although there already exist some location systems, such as those presented in [17] and [18], which can achieve lane-level location performance, these systems require the accurate detection on unique driving events through smart phones or the deployment of lane anchors. So they dramatically depend on the accuracy in real-time event data provided by smart phones, social network and the road-side anchors [19]–[21].

To resolve these drawbacks, a new class of vehicular CP methods has been presented in recent years [12], [22]. Based on vehicle-to-vehicle (V2V), vehicle-to-infrastructure (V2I) communications, and data fusion technologies [10], [23]–[25], CP is able to further enhance the accuracy and the precision performance of the vehicle localization systems. DSRC, with a bandwidth of 75 MHz at the 5.9GHz band, is designed for wireless access in vehicular environment (WAVE) to ensure a maximum communication range up to 1000 m under line-of-sight (LOS) conditions, or up to 300 m under high mobility environments, and to provide the capacity of 50 millisecond-delays on the end-to-end communication and a data rate from 3 to 27 Mb/s [26]. Due to the aforementioned properties, DSRC has become an attractive technology for the CV applications which aim to establish an inter-connected system among intelligent vehicles, and to make incremental improvements in traffic safety, transport efficiency and environmental contaminants. To set up the fundamental framework on the cooperative localization systems, insightful explorations have been presented in [24] and [27] from the fundamental theories to the real world applications, including the theoretical limits, the optimized algorithms and the advanced technologies. Specifically, the field-testing researches indicate that some DSRC-based CP techniques achieving lane-level accuracy can profoundly benefit many applications related to traffic safety [18], [25], [28].

In this paper, we present a framework of DSRC-based enhancement for mobile vehicle localization using the DSRC physical layer data and the coarse position and velocity data provided by the commodity GPS. The enhancement is

achieved by sharing and combining multilateral information of local vehicles through DSRC. The main contributions of this paper are summarized as follows:

- A motion state of each vehicle is represented by its real-time position and velocity. Using the first-order Taylor series approximation, we have developed a linearized system model to formulate the relationship between the real-time vehicular motion state and the physical layer measurements including the DFS and the RSSI, and obtained a transition matrix which reveals the benefit of information interaction among local vehicles into cooperative localization enhancements.
- With the linearized system model aforementioned, we have further proposed a distributed interactive multiple-model (IMM) Kalman filter, which can be applied to track variations of acceleration of vehicles and the covariances of the DFS and the RSSI measurements under the different situations. The Kalman filter is implemented to achieve local information fusion among vehicles in an on-line distributed manner, such that it can enhance the position performance of vehicle localization systems.
- We derive a novel theoretical lower bound limiting the positioning estimation performance, named the mSPEB. The closed-form of the mSPEB needs to process a lower-dimensional equivalent Fisher information matrix (EFIM) and to calculate the bound for the minimum eigenvalue of a high-dimensional Fisher information matrix (FIM), such that it is with lower complexity, when compared to the SPEB used in current literature [14], [29], [30] that has to calculate the inverse of the high-dimensional FIM directly.

The reminder of this paper is organized as follows. The problem to be solved and the analytical models are presented in Section II. The procedure of the data fusion method and the CV-enhanced DIMM-KF algorithm are jointly described in Section III. Numerical results are analyzed and compared in Section IV. Finally, the conclusions are discussed in Section V.

II. SYSTEM MODEL AND LOCALIZATION ENHANCEMENT

The problem to be solved is to estimate the position of a target vehicle (TV) moving on a road section where there are many other moving neighbors around the TV. Assume that a part of participated vehicles in the CV scenarios are able to know their own state information, including position, velocity provided by the GPS receiver. Meanwhile, it should be noted that the neighbors state information is easy to obtain from the DSRC links from which the DFS and the RSSI measurements can be extracted as well. We define CV penetration to represent the percentage of vehicles who hold the CV abilities on the simulated road section. In this scenario, the TV is considered as a research objective for positioning enhancements, and the neighbors are considered as the vehicles who are within the coverage of the DSRC networks of the TV.

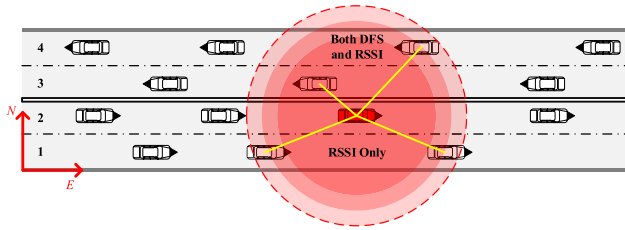


FIGURE 1. Positioning enhanced by the DFS and the RSSI measurements.

A. SYSTEM MODEL

Consider a CV scenario consisting of the moving vehicles, where each vehicle is equipped with a GPS receiver providing coarse data to set up the state vector $\theta_k = [m_{x,k}, m_{y,k}, \dot{m}_{x,k}, \dot{m}_{y,k}]^T$. The position and the velocity components of the vehicle are denoted by $(m_{x,k}, m_{y,k})$ and $(\dot{m}_{x,k}, \dot{m}_{y,k})$, respectively. The x and y subscripts denote the orientation along the East (E) and the North (N) axes, respectively. The subscript k denotes the time step, and T is the transpose operator. The dynamic procedure of the moving vehicles can be considered as the following motion model [31], [32]:

$$\theta_{k+1} = \mathbf{F}\theta_k + \mathbf{G}(\varphi_k + \zeta_k), \tag{1}$$

with

$$\mathbf{F} = \begin{bmatrix} \mathbf{I}_2 & \Delta t \mathbf{I}_2 \\ \mathbf{O}_2 & \mathbf{I}_2 \end{bmatrix}, \quad \varphi_k = \begin{bmatrix} a_{x,k} \\ a_{y,k} \end{bmatrix},$$

$$\mathbf{G} = \begin{bmatrix} \frac{1}{2} \Delta t^2 \mathbf{I}_2 \\ \Delta t \mathbf{I}_2 \end{bmatrix}, \quad \zeta_k = \begin{bmatrix} \zeta_{x,k} \\ \zeta_{y,k} \end{bmatrix}, \tag{2}$$

where φ_k is the discrete-time command process and ζ_k is the system noise modeled as zero-mean Gaussian noise with a covariance matrix \mathbf{Q}_k . \mathbf{F} is the system transition matrix describing the movement of the TV between two consecutive time steps. \mathbf{G} is the transition matrix that models the acceleration-related state and the system noise changes. \mathbf{I}_M denotes a $M \times M$ identity matrix, and \mathbf{O}_M denotes a $M \times M$ zero matrix. Correspondingly, $\zeta_{x,k}$ and $\zeta_{y,k}$ are the acceleration noise along the E and the N axes, respectively, and Δt is the sampling period.

The command process φ_k is a time-homogeneous Markov chain with a finite state space which takes a set of acceleration values $\varphi = \{a_1, \dots, a_L\}$. The transition probability matrix for the different acceleration states in φ is defined as $\Pi^\varphi = [\pi_{pq}^\varphi]$ with the transition probability $\pi_{pq}^\varphi = \mathbb{P}\{\varphi_k = a_p | \varphi_{k-1} = a_q\}$ where $0 \leq \pi_{pq}^\varphi \leq 1$, $\sum_{q=1}^L \pi_{pq}^\varphi = 1$, $p, q = 1, \dots, L$. It should be noted that the system model (1) with Markovian switching systems has been widely used to characterize the state variations of the dynamic object [29], [32], [33]. In the considerable scenario, it is

reasonable to utilize the Markov chain in the model (1) to represent the process that vehicles suffer from sudden changes caused by various traffic incidents, such as stop signs, or traffic lights switching. Moreover, the set φ can be considered as a sectional-continuous function during each instant time interval (the sampling period). Such a model with the acceleration switching among different non-zero means is more effective to characterize the vehicle movements in the real scenario than the motion models only with a zero-mean white Gaussian noise in general [14], [32]–[34]. In terms of the system model described as (1), the measurement model can be defined as follows:

$$\mathbf{z}_k = \mathbf{h}(\theta_k) + \vartheta_k(\phi_k), \tag{3}$$

where $\mathbf{h} = [m_{x,k}, m_{y,k}, \dot{m}_{x,k}, \dot{m}_{y,k}, \rho_k^1, \dots, \rho_k^i, r_k^1, \dots, r_k^j]^T$ is a nonlinear measurement vector associated with θ_k , and ϑ_k is the measurement noise modeled as zero-mean white Gaussian noise with varying covariance matrix \mathbf{R}_k determined by ϕ_k . ϕ_k is a time-homogeneous Markov chain with two states to represent the switching modes $\phi = \{s_1, s_2\}$, where s_1 is assigned to the event ‘‘LOS’’, and s_2 is assigned to the event ‘‘NLOS’’. Correspondingly, the transition probability matrix is defined as $\Pi^\phi = [\pi_{uv}^\phi]$ with transition probability $\pi_{uv}^\phi = \mathbb{P}\{\phi_k = s_u | \phi_{k-1} = s_v\}$, where $0 \leq \pi_{uv}^\phi \leq 1$, $\sum_{v=1}^2 \pi_{uv}^\phi = 1$, $u, v = 1, 2$.

Assume that there are j neighbors within the DSRC coverage of the TV, to whom i of j neighbors are traveling in the opposite direction ($0 \leq i \leq j$). Signals transmitted from these i neighbors can be modeled by the deployment of the DFS measurements. For brief descriptions, we let $N^{DFS} = \{1, 2, \dots, i\}$ denotes the set of the neighbors who provide the DFS measurements, and ρ_k^α denotes that measurements obtained from the neighbor α at the time instant k , $\alpha \in N^{DFS}$, which can be formulated as follows [14]:

$$\rho_k^\alpha = -\frac{f}{c} \frac{d(d_k^\alpha)}{dt} + \vartheta_k^\alpha, \tag{4}$$

$$d_k^\alpha = \sqrt{(m_{x,k} - m_{x,k}^\alpha)^2 + (m_{y,k} - m_{y,k}^\alpha)^2}, \tag{5}$$

where f is the transmission frequency of DSRC, and c is the speed of light. d_k^α is the relative distance between the TV and its neighbor α , and ϑ_k^α is the DFS-related observation noise. Correspondingly, $(m_{x,k}^\alpha, m_{y,k}^\alpha)$ denotes the position of the neighbor α . Substituting (5) into (4), the equation (4) can be reformulated as in (6), as shown at the bottom of this page, where $(\dot{m}_{x,k}^\alpha, \dot{m}_{y,k}^\alpha)$ is the velocity vector of the neighbor α .

Correspondingly, we let $N^{RSSI} = \{1, 2, \dots, j\}$ denote the set of the neighbors who provide the RSSI measurements. The received power r_k^β corresponding to that measurements from the neighbor β at the time instant k , $\beta \in N^{RSSI}$,

$$\rho_k^\alpha = -\frac{f}{c} \left[\frac{(m_{x,k} - m_{x,k}^\alpha)(\dot{m}_{x,k} - \dot{m}_{x,k}^\alpha) + (m_{y,k} - m_{y,k}^\alpha)(\dot{m}_{y,k} - \dot{m}_{y,k}^\alpha)}{\sqrt{(m_{x,k} - m_{x,k}^\alpha)^2 + (m_{y,k} - m_{y,k}^\alpha)^2}} \right] + \vartheta_k^\alpha, \tag{6}$$

is an important metrics obtained from the DSRC physical layer. According to the log-distance path loss model defined in [35] and [36], the laws to model the path-loss behavior of DSRC propagation between vehicles can be formulated as follows:

$$r_k^\beta = C - 10\gamma \lg(d_k^\beta) + \vartheta_k^\beta, \quad (7)$$

$$d_k^\beta = \sqrt{(m_{x,k} - m_{x,k}^\beta)^2 + (m_{y,k} - m_{y,k}^\beta)^2}, \quad (8)$$

where C is a constant with regard to the transmission power and $\gamma \in [2, 5]$ is the path-loss exponent. d_k^β is the relative distance between the TV and its neighbor β , and ϑ_k^β is the RSSI-related measurement noise. Correspondingly, $(m_{x,k}^\beta, m_{y,k}^\beta)$ denotes the position of the neighbor β . The transition process between the LOS and the NLOS conditions could be sharply modeled as a first-order Markov chain with two states $\{s_1, s_2\}$ [32], [34], [37], [38]. As a result, a zero-mean white Gaussian noise is considered with a variance matrix \mathbf{R}_k^{LOS} in the LOS condition whereas a variance matrix \mathbf{R}_k^{NLOS} is employed in the NLOS condition. Specifically, channel modeling in V2V communication environments is a significant issue without concluding a common sense, so the fundamental log-distance path loss model has been used to depict the V2V channel for simplicity.

Note that the set φ and the set ϕ are two independent Markov chains specifying the behavior of the sudden changes of the acceleration and the transition between the LOS and the NLOS conditions, respectively. It should be mentioned that the state metrics in the measurement model depends on the quality of the DSRC links between the TV and its neighbors. Moreover, it is with great probability that the measurement vector consists of the metrics measured from both the LOS and the NLOS conditions. Particularly, the neighbor $\alpha \in N^{DFS}$ could contribute to both the DFS and the RSSI measurements, while the neighbor $\beta \in N^{RSSI}$ could be functionally divided into two portions. One of them following the set $\beta \in N^{RSSI}/N^{DFS}$ could just benefit the RSSI measurements and the other portion could be with the same function as the neighbor $\alpha \in N^{DFS}$.

To solve the nonlinear observation problem presented in model (3), an extended Kalman filter (EKF) method has been used in [14]. Applying the first-order Taylor expansion to (3) around an arbitrary state vector, \mathbf{h} can be transformed to a stereotyped matrix in which all of the components are supposed to obtain from the GPS and the DSRC on-board unit (OBU). Subsequently, the model (3) can be reformulated as follows:

$$\mathbf{z}_k \cong \mathbf{H}_k \theta_k + \vartheta_k(\phi_k), \quad (9)$$

where

$$\mathbf{H}_k = \begin{bmatrix} 1 & 0 & 0 & 0 \\ 0 & 1 & 0 & 0 \\ 0 & 0 & 1 & 0 \\ 0 & 0 & 0 & 1 \\ \mathcal{H}_k^{11} & \mathcal{H}_k^{12} & \mathcal{H}_k^{13} & \mathcal{H}_k^{14} \\ \vdots & \vdots & \vdots & \vdots \\ \mathcal{H}_k^{i1} & \mathcal{H}_k^{i2} & \mathcal{H}_k^{i3} & \mathcal{H}_k^{i4} \\ \mathcal{G}_k^{11} & \mathcal{G}_k^{12} & 0 & 0 \\ \vdots & \vdots & \vdots & \vdots \\ \mathcal{G}_k^{j1} & \mathcal{G}_k^{j2} & 0 & 0 \end{bmatrix}, \quad (10)$$

with the transition components formulated as (11)-(16), as shown in the bottom of this page.

$$\mathcal{H}_k^{\alpha 3} = \frac{\partial \rho_k^\alpha}{\partial \dot{m}_{x,k}} = -\frac{f(m_{x,k} - m_{x,k}^\alpha)}{c d_k^\alpha}, \quad (13)$$

$$\mathcal{H}_k^{\alpha 4} = \frac{\partial \rho_k^\alpha}{\partial \dot{m}_{y,k}} = -\frac{f(m_{y,k} - m_{y,k}^\alpha)}{c d_k^\alpha}, \quad (14)$$

$$\mathcal{G}_k^{\beta 1} = \frac{\partial r_k^\beta(0, 0)}{\partial m_{x,k}} = \frac{10}{\ln 10} \gamma \frac{m_{x,k}^\beta}{(d_k^\beta)^2}, \quad (15)$$

$$\mathcal{G}_k^{\beta 2} = \frac{\partial r_k^\beta(0, 0)}{\partial m_{y,k}} = \frac{10}{\ln 10} \gamma \frac{m_{y,k}^\beta}{(d_k^\beta)^2}. \quad (16)$$

Let r^β be an infinite differentiable function in some open neighborhood around $(m_{x0}, m_{y0}) = (0, 0)$, then according to Multivariate Taylor Expansion theorem, the linear approximation from the Taylor series of $r^\beta(m_x, m_y)$ can be formulated as

$$r^\beta(m_x, m_y) \cong r^\beta(m_{x0}, m_{y0}) + \frac{\partial r^\beta(m_{x0}, m_{y0})}{\partial m_x} (m_x - m_{x0}) + \frac{\partial r^\beta(m_{x0}, m_{y0})}{\partial m_y} (m_y - m_{y0}). \quad (17)$$

After putting into the corresponding point, (17) can be simplified as

$$r^\beta(m_x, m_y) - r^\beta(0, 0) = \frac{\partial r^\beta(0, 0)}{\partial m_x} m_x + \frac{\partial r^\beta(0, 0)}{\partial m_y} m_y. \quad (18)$$

Hence, the RSSI measurements of the measurement model can be linearized into a block matrix, as shown in (10). The similar proof for the DFS measurements is omitted due to the space constraint. It should be noted that the RSSI-related measurements in (9) are not the true value

$$\mathcal{H}_k^{\alpha 1} = \frac{\partial \rho_k^\alpha}{\partial m_{x,k}} = -\frac{f(m_{y,k} - m_{y,k}^\alpha) [(m_{y,k} - m_{y,k}^\alpha)(\dot{m}_{x,k} - \dot{m}_{x,k}^\alpha) - (m_{x,k} - m_{x,k}^\alpha)(\dot{m}_{y,k} - \dot{m}_{y,k}^\alpha)]}{c (d_k^\alpha)^3}, \quad (11)$$

$$\mathcal{H}_k^{\alpha 2} = \frac{\partial \rho_k^\alpha}{\partial m_{y,k}} = -\frac{f(m_{x,k} - m_{x,k}^\alpha) [(m_{x,k} - m_{x,k}^\alpha)(\dot{m}_{y,k} - \dot{m}_{y,k}^\alpha) - (m_{y,k} - m_{y,k}^\alpha)(\dot{m}_{x,k} - \dot{m}_{x,k}^\alpha)]}{c (d_k^\alpha)^3}, \quad (12)$$

measured at the receiver, but are the value calculated by the left hand of the equation (18) which is the result of the true RSSI measurements minus the value of $r^\beta(m_x, m_y)$ at $(m_x = 0, m_y = 0)$.

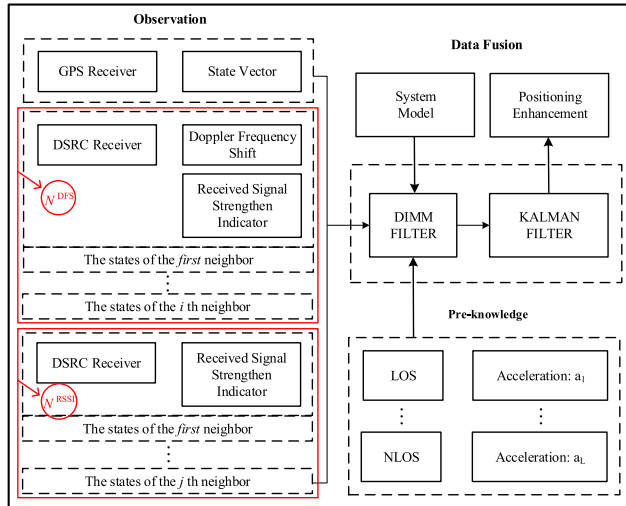


FIGURE 2. The schematic of the proposed vehicular cooperative localization method.

B. THE CV-ENHANCED DIMM-KF FOR MOBILE VEHICLE LOCALIZATION

The schematic of the CV-enhanced vehicle localization method is shown in Fig. 2. The proposed CV-enhanced DIMM-KF algorithm handling two switching parameters in (1) and (9) works as follows:

Step 1) Mixing probabilities calculation

$$\mu_{k+1,l|s} = \mu_{k+1,p|q}^\phi \mu_{k+1,u|v}^\phi, \tag{19}$$

$$\begin{cases} \mu_{k+1,p|q}^\phi = \pi_{pq}^\phi \mu_{k,p}^\phi / c_q^\phi \\ \mu_{k+1,u|v}^\phi = \pi_{uv}^\phi \mu_{k,u}^\phi / c_v^\phi \end{cases} \tag{20}$$

where $\mu_{k+1,p|q}^\phi$ and $\mu_{k+1,u|v}^\phi$ are defined as the mixing probabilities which are common in the conventional IMM estimator. Both of them can be obtained from (20), where $l, s = 1, 2, \dots, 2L$. In (20), π_{pq}^ϕ and π_{uv}^ϕ represent the transition probabilities of the two aforementioned independent Markov chains, and $\mu_{k,p}^\phi$ and $\mu_{k,u}^\phi$ are the probabilities of the event that the p th motion model and the u th channel mode are in effect at the time step k , respectively, where $p, q = 1, 2, \dots, L$, corresponding to the p, q th mode of the Markov chain ϕ , and $u, v = 1, 2$, corresponding to the u, v th mode of the Markov chain ϕ . Consequently, the normalized constant can be formulated as

$$c_s = c_q^\phi c_v^\phi, \tag{21}$$

where c_q^ϕ and c_v^ϕ are the distributed normalized constants for different Markov chains with the formulation as

$$\begin{cases} c_q^\phi = \sum_{p=1}^L \{\pi_{pq}^\phi \mu_{k,p}^\phi\} \\ c_v^\phi = \sum_{u=1}^2 \{\pi_{uv}^\phi \mu_{k,u}^\phi\}. \end{cases} \tag{22}$$

Step 2) Interaction

Mixing the state estimations and the covariance matrices according to the following equations (23) and (24), respectively,

$$\theta_{k|k,s}^0 = \sum_{p=1}^L \left\{ \mu_{k+1,p|q}^\phi \sum_{u=1}^2 \left\{ \mu_{k+1,u|v}^\phi \theta_{k|k,p,u}^{0,0} \right\} \right\}, \tag{23}$$

$$\mathbf{P}_{k|k,s}^0 = \sum_{p=1}^L \left\{ \begin{aligned} &\mu_{k+1,p|q}^\phi \\ &\times \left\{ \mathbf{P}_{k|k,p,v}^{0,0} + \left\{ \theta_{k|k,p,v}^{0,0} - \theta_{k|k,s}^0 \right\} \right\} \\ &\times \left\{ \theta_{k|k,p,v}^{0,0} - \theta_{k|k,s}^0 \right\}^T \end{aligned} \right\}, \tag{24}$$

where

$$\mathbf{P}_{k|k,p,v}^{0,0} = \sum_{u=1}^2 \left\{ \begin{aligned} &\mu_{k+1,u|v}^\phi \\ &\times \left\{ \mathbf{P}_{k|k,p,u}^{0,0} + \left\{ \theta_{k|k,p,u}^{0,0} - \theta_{k|k,p,v}^0 \right\} \right\} \\ &\times \left\{ \theta_{k|k,p,u}^{0,0} - \theta_{k|k,p,v}^0 \right\}^T \end{aligned} \right\}. \tag{25}$$

Step 3) Mode update and prediction steps

Calculate $\mathcal{H}_k^{\alpha 1}, \dots, \mathcal{H}_k^{\alpha 4}, \mathcal{G}_k^{\beta 1}, \mathcal{G}_k^{\beta 2}$, according to the equations (11)-(16) and then update the measurement transition matrix \mathbf{H}_k defined by (10) associated with the CV technologies.

The CV-enhanced DIMM-KF gain is given by

$$\mathbf{K}_k = \mathbf{P}_{k|k-1,s} \mathbf{H}_k^T \times \{\mathbf{H}_k \mathbf{P}_{k|k-1,s} \mathbf{H}_k^T + \mathbf{R}_k\}^{-1}. \tag{26}$$

The update steps of the CV-enhanced DIMM-KF are given by

$$\theta_{k|k,s} = \theta_{k|k-1,s} + \mathbf{K}_k \{\mathbf{z}_k - \mathbf{H}_k \theta_{k|k-1,s}\}, \tag{27}$$

$$\mathbf{P}_{k|k,s} = \mathbf{P}_{k|k-1,s} - \mathbf{K}_k \{\mathbf{H}_k \mathbf{P}_{k|k-1,s} \mathbf{H}_k^T + \mathbf{R}_k\} \mathbf{K}_k^T. \tag{28}$$

The prediction steps of the CV-enhanced DIMM-KF are given by

$$\theta_{k+1|k,s} = \mathbf{F} \theta_{k|k,s}^0 + \mathbf{G} \varphi_{k,s}, \tag{29}$$

$$\mathbf{P}_{k+1|k,s} = \mathbf{F} \mathbf{P}_{k|k,s}^0 \mathbf{F}^T + \mathbf{G} \mathbf{Q} \mathbf{G}^T. \tag{30}$$

The likelihood function $\Lambda_{k,t}$ and the prediction mode probability $\mu_{k,t}$ are formulated as

$$\Lambda_{k,s} = normal(\mathbf{z}_k - \mathbf{H}_k \theta_{k|k-1,s}; 0, \mathbf{H}_k \mathbf{P}_{k|k-1,s} \mathbf{H}_k^T + \mathbf{R}_k). \tag{31}$$

Step 4) Mode probability update

The probability at the time step k is calculated as

$$\mu_{k,s} = \Lambda_{k,s} c_s / c, \tag{32}$$

where c is the overall normalized constant defined as

$$c = \sum_{s=1}^{2L} \lambda_{k,s} c_s. \tag{33}$$

Algorithm 1 One Trial of the CV-Enhanced DIMM-KF Algorithm

Require: $\theta_{k|k,p,u}^{0,0}$, $\theta_{k|k,p,v}^{0,0}$, $\mathbf{P}_{k|k,p,u}^{0,0}$, $\mu_{k+1,p|q}^\varphi$, $\mu_{k+1,u|v}^\phi$, π_{pq}^φ , π_{uv}^ϕ , the GPS, the DFS, and the RSSI measurements \mathbf{z}_k^{GPS} , \mathbf{z}_k^{DFS} , \mathbf{z}_k^{RSSI}

- 1: Initial c_q^φ , c_v^ϕ , $\mu_{k+1,p|q}^\varphi$, $\mu_{k+1,u|v}^\phi$, $\theta_{k|k,s}^0$, and $\mathbf{P}_{k|k,s}^0$
- 2: **for** $q = 1, \dots, L$ **do**
- 3: **for** $p = 1, \dots, L$ **do**
- 4: Calculate c_q^φ and $\mu_{k+1,p|q}^\varphi$ via (22) and (20), respectively
- 5: **end for**
- 6: **end for**
- 7: **for** $v = 1, 2$ **do**
- 8: **for** $u = 1, 2$ **do**
- 9: Calculate c_v^ϕ and $\mu_{k+1,u|v}^\phi$ via (22) and (20), respectively
- 10: **end for**
- 11: **end for**
- 12: **for** $s = 1, \dots, 2L$ **do**
- 13: **for** $l = 1, \dots, 2L$ **do**
- 14: Calculate $\theta_{k|k,s}^0$ and $\mathbf{P}_{k|k,s}^0$ via (23)-(25)
- 15: **end for**
- 16: **end for**
- 17: Calculate $\mathcal{H}_k^{\alpha 1}, \dots, \mathcal{H}_k^{\alpha 4}, \mathcal{G}_k^{\beta 1}, \mathcal{G}_k^{\beta 2}$ via (11)-(16)
- 18: Set \mathbf{H}_k via (10) and set \mathbf{R}_k according to the number of the neighbors in $N_{DFS} \cup N_{RSSI}$ \triangleright CV-enhanced
- 19: **for** $s = 1, \dots, 2L$ **do** \triangleright The DIMM Kalman Filter
- 20: Update $\theta_{k|k,s}$ and $\mathbf{P}_{k|k,s}$ via (26)-(28)
- 21: Predict $\theta_{k+1|k,s}$ and $\mathbf{P}_{k+1|k,s}$ via (29)-(30)
- 22: **end for**
- 23: Combine $\theta_{k|k}$ and $\mathbf{P}_{k|k}$ via (34)-(35).

Step 5) Combination

In the final stage, the CV-enhanced DIMM-KF algorithm combines the state estimations and the covariance matrices as the following manners:

$$\theta_{k|k} = \sum_{s=1}^{2L} \mu_{k,s} \theta_{k|k,s}, \tag{34}$$

$$\mathbf{P}_{k|k} = \sum_{s=1}^{2L} \mu_{k,s} \times \left\{ \mathbf{P}_{k|k,s} + \{ \theta_{k|k,s} - \theta_{k|k} \} \{ \theta_{k|k,s} - \theta_{k|k} \}^T \right\}. \tag{35}$$

The overall CV-enhanced DIMM-KF algorithm is described in Algorithm 1.

III. GENERAL PERFORMANCE ANALYSIS

In this section, we briefly review the information inequality, describe the framework for the designed general measurements containing the positioning-related information, and study a tight computational method of the fundamental limits on the positioning metrics which is defined as the square position error bound (SPEB) in principle [39]. Subsequently,

we transform the problem of estimation of the theoretical bound to that of analyzing the bound for the trace of the inverse matrix, propose a novel lower bound limiting the positioning estimation performance, named the mSPEB, which reduces the computation complexity compared to the calculation of the SPEB, and finally formulate the Fisher information matrix (FIM) of the system model for studying the estimated covariance lower bound of the CV-enhanced positioning.

Throughout this section, Ξ denotes an \mathcal{N} -by- \mathcal{N} symmetric positive definite matrix with eigenvalues

$$\lambda_1 \leq \lambda_2 \leq \dots \leq \lambda_{\mathcal{N}}.$$

$\lambda(\Xi)$ is the set of all eigenvalues. The parameters \mathcal{S} and \mathcal{T} denote the bounds for the lowest and largest eigenvalues λ_1 and $\lambda_{\mathcal{N}}$ of Ξ .

$$0 \leq \mathcal{S} \leq \lambda_1, \lambda_{\mathcal{N}} \leq \mathcal{T}.$$

$\text{TR}(\cdot)$ is the trace operator and $\|\cdot\|_F^2$ is the F-norm operator.

A. CRLB

To analyze the optimal theoretical performance of an unbiased estimator, the Cramér-Rao lower bound (CRLB) is commonly regarded as the evaluation benchmark [29], [40]. Note that the variance's equality with the mean squared error (MSE) for the estimator $\hat{\Phi}$ strictly satisfies the information inequality [41],

$$\mathbb{E}\{(\hat{\Phi} - \Phi)(\hat{\Phi} - \Phi)^T\} \geq \mathbf{I}(\Phi)^{-1}, \tag{36}$$

where $\mathbf{I}(\Phi)$ is the FIM for the parameter vector Φ . However, the parameters we interested in are merely the positioning-related error variance, which indicates that only the upper left 2×2 submatrix of $\mathbf{I}(\Phi)^{-1}$ is of interest in a 2-D localization problem.

B. SPEB

The square position error bound (SPEB), a measure to bound the average squared position error, is commonly defined to evaluate the performance of localization accuracy on wireless collaboration networks [39]. Determining the SPEB requires to obtain the inversion of the FIM as follows:

$$\text{SPEB} = \text{TR}\{\mathbf{I}(\Phi)^{-1}\}_{2 \times 2} = \mathbf{I}(\Phi)^{-1}(1, 1) + \mathbf{I}(\Phi)^{-1}(2, 2). \tag{37}$$

However, by reason of $\mathbf{I}(\Phi)$ usually being a high-dimension matrix, the inversion of $\mathbf{I}(\Phi)$ is quite complex to calculate, which results a tradeoff between computation complexity and performance evaluation. In fact, only the submatrix $[\mathbf{I}(\Phi)^{-1}]_{2 \times 2}$ can contribute the unique insights into the bounding laws on the localization problems.

C. EFIM

In order to circumvent the calculation of the matrix inversion, we firstly introduce the notions of the equivalent Fisher Information Matrix (EFIM) [39].

Given a parameter vector $\Phi = [\Phi_\Omega^T, \Phi_\Upsilon^T]^T$ and let the FIM $\mathbf{I}(\Phi)$ be written as a 2×2 block matrix

$$\mathbf{I}(\Phi) = \begin{pmatrix} \mathbf{I}_\Omega & \mathbf{I}_{\Omega\Upsilon} \\ \mathbf{I}_{\Omega\Upsilon}^T & \mathbf{I}_\Upsilon \end{pmatrix}, \quad (38)$$

where $\Phi \in \mathbb{R}^{\mathcal{N}}$ and $\Phi_\Omega \in \mathbb{R}^{\mathcal{M}}$. $\mathbf{I}_\Omega \in \mathbb{R}^{\mathcal{M} \times \mathcal{M}}$ represents the partial information of $\mathbf{I}(\Phi)$ only pertaining to Ω , $\mathbf{I}_\Upsilon \in \mathbb{R}^{(\mathcal{N}-\mathcal{M}) \times (\mathcal{N}-\mathcal{M})}$ represents the partial information of $\mathbf{I}(\Phi)$ only pertaining to Υ , and $\mathbf{I}_{\Omega\Upsilon} \in \mathbb{R}^{\mathcal{M} \times (\mathcal{N}-\mathcal{M})}$ represents the coupled information between Ω and Υ , while the notions corresponding to the dimension meet the conditions that $1 \leq \mathcal{M} \leq \mathcal{N}$. Consequently, we obtain the EFIM of Ω as follows:

$$\mathbf{I}(\Phi_\Omega) = \mathbf{I}_\Omega - \mathbf{I}_{\Omega\Upsilon} \mathbf{I}_\Upsilon^{-1} \mathbf{I}_{\Omega\Upsilon}^T. \quad (39)$$

The right hand of (39) is also known as the Schur complement of the sub-block \mathbf{I}_Υ in $\mathbf{I}(\Phi)$ [42], which is equivalent to $\mathbf{I}(\Phi)$ for the parameters Φ_Ω in the sense that it retains all the necessary information to deduce the CRLB of Ω :

$$\left[\mathbf{I}(\Phi)^{-1} \right]_\Omega = \left[\mathbf{I}(\Phi_\Omega)^{-1} \right]. \quad (40)$$

D. THE m SPEB

A novel theoretical lower bound of the MSE matrix of an unbiased positioning-related estimator is derived through studying the properties from the bounds for the trace of the inverse of a symmetric positive definite matrix.

Theorem 1: Given a cooperative localization network with parameter vectors Φ and $\Phi = [\Phi_\Omega^T, \Phi_\Upsilon^T]^T$ where Φ_Ω is the position information vector and Φ_Υ is the other parameter vector independent of the position information. In a positioning estimation problem, if the corresponding FIM for the parameter vector Φ , $\mathbf{I}(\Phi)$, is a positive definite matrix, then a lower bound of SPEB is given by

$$\text{SPEB} \geq \frac{-\bar{\tau}^2 \mathcal{M}^2 + (\bar{\mu}_1 \bar{\tau} + \bar{\mu}_2) \mathcal{M} - \bar{\mu}_1^2}{\bar{\mu}_2 \bar{\tau} - \bar{\mu}_1 \bar{\tau}^2}, \quad (41)$$

where $\bar{\mu}_1 = \text{TR}(\mathbf{I}(\Phi_\Omega))$, $\bar{\mu}_2 = \|\mathbf{I}(\Phi_\Omega)\|_F^2$, $\bar{\tau}$ is the upper bound of eigenvalues of $\mathbf{I}(\Phi_\Omega)$, and \mathcal{M} is the dimension of $\mathbf{I}(\Phi_\Omega)$. $\mathbf{I}(\Phi_\Omega)$ is the corresponding EFIM.

Proof: The Schur complement condition on positive definite matrix states that for any symmetric matrix Σ of the form

$$\Sigma = \begin{pmatrix} \mathbf{A} & \mathbf{B} \\ \mathbf{B}^T & \mathbf{C} \end{pmatrix},$$

if \mathbf{C} is invertible, the following property will be obtained:

$$\Sigma \succ 0 \iff \mathbf{A} - \mathbf{B}\mathbf{C}^{-1}\mathbf{B}^T \succ 0 \text{ and } \mathbf{C} \succ 0 \quad (42)$$

where $\Sigma \succ 0$ meaning that Σ is a positive definite matrix. In a specified positioning estimation problem, it is clear from (42) that the corresponding EFIM, $\mathbf{I}(\Phi_\Omega)$, is a positive definite matrix as long as the corresponding FIM, $\mathbf{I}(\Phi)$, is a positive definite matrix.

Having shown that the lower bound for the SPEB is a function of the parameters of the EFIM, $\mathbf{I}(\Phi_\Omega)$, including the

trace, the F-norm, the upper bound of eigenvalues, and the dimension, we will explain the obtained result by introducing a Lemma which derives the lower and upper bounds for the trace of the inverse of a symmetric positive definite matrix presented by Bai and Golub in [43].

Lemma 1: Let Ξ be an $\mathcal{N} \times \mathcal{N}$ symmetric positive definite matrix, $\mu_1 = \text{TR}(\Xi)$, $\mu_2 = \|\Xi\|_F^2$ and $\lambda(\Xi) \subset [\mathcal{S}, \mathcal{T}]$ with $\mathcal{S} > 0$, then

$$\begin{aligned} & [\mu_1 \ \mathcal{N}] \begin{bmatrix} \mu_2 & \mu_1 \\ \mathcal{T}^2 & \mathcal{T} \end{bmatrix}^{-1} \begin{bmatrix} \mathcal{N} \\ 1 \end{bmatrix} \\ & \leq \text{TR}(\Xi^{-1}) \leq [\mu_1 \ \mathcal{N}] \begin{bmatrix} \mu_2 & \mu_1 \\ \mathcal{S}^2 & \mathcal{S} \end{bmatrix}^{-1} \begin{bmatrix} \mathcal{N} \\ 1 \end{bmatrix}. \end{aligned} \quad (43)$$

In addition, it is obvious that the FIM, $\mathbf{I}(\Phi)$, is a symmetric matrix. Consequently, in a specified position estimation problem, if the corresponding FIM is a positive definite matrix, both the FIM, $\mathbf{I}(\Phi)$, and the EFIM, $\mathbf{I}(\Phi_\Omega)$, are symmetric positive definite matrix, so all the preconditions of the Lemma are met. Now, we can use the Lemma above with $\Xi = \mathbf{I}(\Phi)$. Noted that the SPEB of the FIM, $\mathbf{I}(\Phi)$, is $\text{TR}(\mathbf{I}(\Phi_\Omega)^{-1})$, and the dimension of the EFIM, $\mathbf{I}(\Phi_\Omega)$, is \mathcal{M} . Expanding the left hand of the inequality (43) in (44), our end result is concluded in (41).

$$\begin{aligned} & [\mu_1 \ \mathcal{N}] \begin{bmatrix} \mu_2 & \mu_1 \\ \mathcal{T}^2 & \mathcal{T} \end{bmatrix}^{-1} \begin{bmatrix} \mathcal{N} \\ 1 \end{bmatrix} \\ & = \frac{-\mathcal{T}^2 \mathcal{N}^2 + (\mu_1 \mathcal{T} + \mu_2) \mathcal{N} - \mu_1^2}{\mu_2 \mathcal{T} - \mu_1 \mathcal{T}^2}. \end{aligned} \quad (44)$$

Theorem 2: Given a cooperative localization network with parameter vectors Φ and $\Phi = [\Phi_\Omega^T, \Phi_\Upsilon^T]^T$ where Φ_Ω is the position information vector and Φ_Υ is the other parameter vector independent of the position information. In a positioning estimation problem, if the corresponding FIM for the parameter vector Φ , $\mathbf{I}(\Phi)$, is a positive definite matrix, then a lower bound of SPEB is given by

$$\text{SPEB} \geq \frac{\mathcal{M}}{\bar{\mathcal{S}}} + \sum_{\mathcal{I}=1}^{\mathcal{M}} \frac{(\bar{\mathcal{S}} - \Gamma_{\mathcal{I}\mathcal{I}})^2}{\bar{\mathcal{S}}(\bar{\mathcal{S}}\Gamma_{\mathcal{I}\mathcal{I}} - \mathcal{W}_{\mathcal{I}\mathcal{I}})}, \quad (45)$$

where $\bar{\mathcal{S}}$ is the lower bound of eigenvalues of $\mathbf{I}(\Phi)$, $\mathcal{W}_{\mathcal{I}\mathcal{I}} = \sum_{\mathcal{J}=1}^{\mathcal{N}} \Gamma_{\mathcal{I}\mathcal{J}}^2$, $\Gamma_{\mathcal{I}\mathcal{J}}$ is the \mathcal{I}, \mathcal{J} th element of $\mathbf{I}(\Phi)$ ($\mathcal{I} = 1, 2, \dots, \mathcal{M}$, $\mathcal{J} = 1, 2, \dots, \mathcal{N}$), \mathcal{N} is the dimension of $\mathbf{I}(\Phi)$, and \mathcal{M} is the dimension of $\mathbf{I}(\Phi_\Omega)$. $\mathbf{I}(\Phi_\Omega)$ is the corresponding EFIM.

Proof: Similar to the proof procedures discussed in the Theorem 1, it is concluded that in a specified positioning estimation problem the corresponding FIM, $\mathbf{I}(\Phi)$, is a symmetric positive definite matrix when the FIM meets the conditions defined in the Theorem 2.

Having shown that the lower bound for the SPEB is a function of the parameter of the FIM, $\mathbf{I}(\Phi)$, including the lower bound of eigenvalues, the entries on the main diagonal, the sum of the entries on the \mathcal{I} th row, and the dimension of the FIM as well as the dimension of EFIM, $\mathbf{I}(\Phi_\Omega)$, we will explain the obtained result by introducing another Lemma

which derives the lower and upper bounds for the entries on its main diagonal of the inverse of a symmetric positive definite matrix presented by Robinson and Wathen in [44].

Lemma 2: Let Ξ be an $\mathcal{N} - \text{by} - \mathcal{N}$ symmetric positive definite matrix, and $\lambda(\Xi) \subset [\mathcal{S}, \mathcal{T}]$ with $\mathcal{S} > 0$, then

$$\frac{1}{\mathcal{S}} + \frac{(\mathcal{S} - \Gamma_{\mathcal{I}\mathcal{I}})^2}{\mathcal{S}(\mathcal{S}\Gamma_{\mathcal{I}\mathcal{I}} - \mathcal{W}_{\mathcal{I}\mathcal{I}})} \leq (\Xi^{-1})_{\mathcal{I}\mathcal{I}} \leq \frac{1}{\mathcal{T}} + \frac{(\mathcal{T} - \Gamma_{\mathcal{I}\mathcal{I}})^2}{\mathcal{T}(\mathcal{T}\Gamma_{\mathcal{I}\mathcal{I}} - \mathcal{W}_{\mathcal{I}\mathcal{I}})}, \quad (46)$$

where $\mathcal{W}_{\mathcal{I}\mathcal{I}} = \sum_{\mathcal{J}=1}^{\mathcal{N}} \Gamma_{\mathcal{I}\mathcal{J}}^2$ and $\Gamma_{\mathcal{I}\mathcal{J}}$ is the \mathcal{I}, \mathcal{J} th element of Ξ ($\mathcal{I}, \mathcal{J} = 1, 2, \dots, \mathcal{N}$).

As we know $\text{TR}(\Xi^{-1}) = \sum_{\mathcal{I}=1}^{\mathcal{N}} (\Xi^{-1})_{\mathcal{I}\mathcal{I}}$, so the lower bound of $\text{TR}(\Xi^{-1})$ can be written as follows:

$$\sum_{\mathcal{I}=1}^{\mathcal{N}} (\Xi^{-1})_{\mathcal{I}\mathcal{I}} \geq \sum_{\mathcal{I}=1}^{\mathcal{N}} \left\{ \frac{1}{\mathcal{S}} + \frac{(\mathcal{S} - \Gamma_{\mathcal{I}\mathcal{I}})^2}{\mathcal{S}(\mathcal{S}\Gamma_{\mathcal{I}\mathcal{I}} - \mathcal{W}_{\mathcal{I}\mathcal{I}})} \right\}. \quad (47)$$

Now, setting the dimension \mathcal{N} to \mathcal{M} , the left hand of (47) is the SPEB, then the end result is concluded. ■

It is noted that the two proposed theorems are suitable for both 2-D and 3-D localization scenarios in general. For a specified 2-D positioning problem, the dimension of the EFIM, \mathcal{M} , is set to 2, while for the 3-D, $\mathcal{M} = 3$.

Lemma 3: Given a cooperative localization network with parameter vectors Φ and $\Phi = [\Phi_{\Omega}^T, \Phi_{\Upsilon}^T]^T$ where Φ_{Ω} is the position information vector and Φ_{Υ} is the other parameter vector independent of the position information. In a positioning estimation problem, if the corresponding FIM for the parameter vector Φ , $\mathbf{I}(\Phi)$, is a positive definite matrix, the resulting theoretical mSPEB—the modified lower bound of the MSE matrix of an unbiased estimator of Φ_{Ω} can be expressed as

$$mSPEB = \max \left\{ \frac{-\bar{\mathcal{T}}^2 \mathcal{M}^2 + (\bar{\mu}_1 \bar{\mathcal{T}} + \bar{\mu}_2) \mathcal{M} - \bar{\mu}_1^2}{\bar{\mu}_2 \bar{\mathcal{T}} - \bar{\mu}_1 \bar{\mathcal{T}}^2}, \frac{\mathcal{M}}{\mathcal{S}} + \sum_{\mathcal{I}=1}^{\mathcal{M}} \frac{(\bar{\mathcal{S}} - \Gamma_{\mathcal{I}\mathcal{I}})^2}{\bar{\mathcal{S}}(\mathcal{S}\Gamma_{\mathcal{I}\mathcal{I}} - \mathcal{W}_{\mathcal{I}\mathcal{I}})} \right\}, \quad (48)$$

where $\bar{\mu}_1 = \text{TR}(\mathbf{I}(\Phi_{\Omega}))$, $\bar{\mu}_2 = \|\mathbf{I}(\Phi_{\Omega})\|_F^2$, $\bar{\mathcal{S}}$ is the lower bound of eigenvalues of $\mathbf{I}(\Phi)$, $\bar{\mathcal{T}}$ is the upper bound of eigenvalues of $\mathbf{I}(\Phi)$, $\mathcal{W}_{\mathcal{I}\mathcal{I}} = \sum_{\mathcal{J}=1}^{\mathcal{N}} \Gamma_{\mathcal{I}\mathcal{J}}^2$, $\Gamma_{\mathcal{I}\mathcal{J}}$ is the \mathcal{I}, \mathcal{J} th element of $\mathbf{I}(\Phi)$ ($\mathcal{I} = 1, 2, \dots, \mathcal{M}$, $\mathcal{J} = 1, 2, \dots, \mathcal{N}$), \mathcal{N} is the dimension of $\mathbf{I}(\Phi)$, and \mathcal{M} is the dimension of $\mathbf{I}(\Phi_{\Omega})$. $\mathbf{I}(\Phi_{\Omega})$ is the corresponding EFIM.

Proof: According to the proof procedures discussed in Theorem 1 and Theorem 2, it is obvious that $SPEB \geq mSPEB$, so the end result is concluded. ■

It should be mentioned that the closed-form of the mSPEB needs to process a lower-dimensional EFIM and to calculate the bound for the minimum eigenvalue of a high-dimensional FIM, such that it is with lower complexity, when compared to the SPEB used in current literature [14], [29], [30] that has to calculate the inverse of the high-dimensional FIM directly.

E. INSIGHTS INTO FACTORS AFFECTING THE CP PERFORMANCE

In this paper, the FIM can be calculated at each time instant k as

$$\mathbf{I}(\theta) = \mathbb{E} \left\{ \left[\frac{\partial \ln(f(\mathbf{z}|\theta))}{\partial \theta} \right] \left[\frac{\partial \ln(f(\mathbf{z}|\theta))}{\partial \theta} \right]^T \right\} = -\mathbb{E} \left\{ \frac{\partial^2 \ln(f(\mathbf{z}|\theta))}{\partial \theta^2} \right\}, \quad (49)$$

where \mathbf{z} is the measurement vector in (9), θ the state vector in (1), $\mathbb{E}\{\cdot\}$ is the expectation operator, and $f\{\cdot\}$ is the conditional Probability Distribution Function (PDF) of \mathbf{z} on condition of the value of θ . Assume that $f(\mathbf{z}|\theta)$ follows a Gaussian distribution $normal(\mathbf{z}; \mathbf{z}_{mean}, \mathbf{R})$ as

$$f(\mathbf{z}|\theta) = \frac{\text{EXP}\{-\frac{1}{2}(\mathbf{z} - \mathbf{z}_{mean})^T \mathbf{R}^{-1}(\mathbf{z} - \mathbf{z}_{mean})\}}{(2\pi)^{\frac{4+i+j}{2}} \sqrt{\text{DET}(\mathbf{R})}}, \quad (50)$$

where the variable \mathbf{z} is normally distributed with the mean \mathbf{z}_{mean} and the covariance matrix \mathbf{R} , i is the total number of the neighbors associated with the DFS measurements, and j is the total number of the neighbors associated with the RSSI measurements. After deploying the natural logarithm on both sides of (50), the formula can be rewritten as

$$\ln(f(\mathbf{z}|\theta)) = -\frac{1}{2} \ln(|\mathbf{R}|) - \frac{1}{2}(\mathbf{z} - \mathbf{z}_{mean})^T \mathbf{R}^{-1}(\mathbf{z} - \mathbf{z}_{mean}) - \frac{4+i+j}{2} \ln(2\pi). \quad (51)$$

Then, substituting (9) into (51), the result of the second-order partial derivative of the state vector θ can be written as

$$\frac{\partial^2 \ln(f(\mathbf{z}|\theta))}{\partial \theta^2} = -\mathbf{H}^T \mathbf{R}^{-1} \mathbf{H}. \quad (52)$$

Subsequently, substituting (52) into (49), the form of the FIM $\mathbf{I}(\theta)$ can be simplified as follows:

$$\mathbf{I}(\theta) = \mathbf{H}^T \mathbf{R}^{-1} \mathbf{H}, \quad (53)$$

which can be formulated with the form of a block matrix as follows:

$$\mathbf{I}(\theta) = \begin{bmatrix} \mathbf{I}_A & \mathbf{I}_B \\ \mathbf{I}_B^T & \mathbf{I}_C \end{bmatrix}. \quad (54)$$

The elements of $\mathbf{I}(\theta)$ are given by (55)-(57), as shown at the top of the next page, where $\sigma_{m_x}, \sigma_{m_y}, \sigma_{\dot{m}_x}, \sigma_{\dot{m}_y}, \sigma_{\rho}, \sigma_r$ are the elements in the covariance matrix of the measurements defined in (58)-(59). Consequently, the mSPEB of $\mathbf{I}(\theta)$ can be obtained from (48). \mathbf{I}_A characterizes the localization information corresponding to the cooperation via inter-vehicle measurements using the GPS and the RSSI-related data, while \mathbf{I}_B and \mathbf{I}_C characterize the same type of measurements using only the GPS data. As the components of each element derived in the FIM, $\mathbf{I}(\theta)$, we can conclude that each inter-vehicle measurement or metrics will contribute to positioning enhancements from the point view of the CRLB.

$$\mathbb{E}_{\mathbf{A}} = \begin{bmatrix} \frac{1}{\sigma_{m_x}^2} + \frac{1}{\sigma_\rho^2} \sum_{\alpha=1}^i (\mathcal{H}_k^{\alpha 1})^2 + \frac{1}{\sigma_r^2} \sum_{\beta=1}^j (\mathcal{G}_k^{\beta 1})^2 & \frac{1}{\sigma_\rho^2} \sum_{\alpha=1}^i (\mathcal{H}_k^{\alpha 1} \mathcal{H}_k^{\alpha 2}) + \frac{1}{\sigma_r^2} \sum_{\beta=1}^j (\mathcal{G}_k^{\beta 1} \mathcal{G}_k^{\beta 2}) \\ \frac{1}{\sigma_\rho^2} \sum_{\alpha=1}^i (\mathcal{H}_k^{\alpha 1} \mathcal{H}_k^{\alpha 2}) + \frac{1}{\sigma_r^2} \sum_{\beta=1}^j (\mathcal{G}_k^{\beta 1} \mathcal{G}_k^{\beta 2}) & \frac{1}{\sigma_{m_y}^2} + \frac{1}{\sigma_\rho^2} \sum_{\alpha=1}^i (\mathcal{H}_k^{\alpha 2})^2 + \frac{1}{\sigma_r^2} \sum_{\beta=1}^j (\mathcal{G}_k^{\beta 2})^2 \end{bmatrix}, \quad (55)$$

$$\mathbb{E}_{\mathbf{B}} = \begin{bmatrix} \frac{1}{\sigma_\rho^2} \sum_{\alpha=1}^i (\mathcal{H}_k^{\alpha 1} \mathcal{H}_k^{\alpha 3}) & \frac{1}{\sigma_\rho^2} \sum_{\alpha=1}^i (\mathcal{H}_k^{\alpha 1} \mathcal{H}_k^{\alpha 4}) \\ \frac{1}{\sigma_\rho^2} \sum_{\alpha=1}^i (\mathcal{H}_k^{\alpha 2} \mathcal{H}_k^{\alpha 3}) & \frac{1}{\sigma_\rho^2} \sum_{\alpha=1}^i (\mathcal{H}_k^{\alpha 2} \mathcal{H}_k^{\alpha 4}) \end{bmatrix}, \quad (56)$$

$$\mathbb{E}_{\mathbf{C}} = \begin{bmatrix} \frac{1}{\sigma_{m_x}^2} + \frac{1}{\sigma_\rho^2} \sum_{\alpha=1}^i (\mathcal{H}_k^{\alpha 3})^2 & \frac{1}{\sigma_\rho^2} \sum_{\alpha=1}^i (\mathcal{H}_k^{\alpha 3} \mathcal{H}_k^{\alpha 4}) \\ \frac{1}{\sigma_\rho^2} \sum_{\alpha=1}^i (\mathcal{H}_k^{\alpha 3} \mathcal{H}_k^{\alpha 4}) & \frac{1}{\sigma_{m_y}^2} + \frac{1}{\sigma_\rho^2} \sum_{\alpha=1}^i (\mathcal{H}_k^{\alpha 4})^2 \end{bmatrix}. \quad (57)$$

IV. NUMERICAL RESULTS

This section discusses a series of computer simulations used to evaluate the performance of the proposed CP method. Meanwhile, the insightful data analyses were conducted to interpret the inherent relationship between traffic incidents and positioning enhancements for mobile vehicle localization.

A. SIMULATION SETUP

Consider a section of urban roads with a width of four lanes (each lane with a width of 3.5 m) and a length of one kilometer. It is assumed that the basic traffic setting is subject to the following conditions: 1) the traffic intensity of the road is 20 vehicle/km, 2) the CV penetration is 100%, and 3) the average velocity of the traffic flow is 90 km/h. The vehicles' dynamics are described by the model (1), and the sampling period $\Delta t = 0.2$ s. The distribution of the system noise ζ_k takes with covariance $\mathbf{Q}_k = \text{diag}(\sigma_{a_{x,k}}^2, \sigma_{a_{y,k}}^2)$, where

the elements $\sigma_{a_{x,k}} = \sqrt{\frac{0.99}{2}} m/s^2$ and $\sigma_{a_{y,k}} = \sqrt{\frac{0.01}{2}} m/s^2$

are the acceleration noise along the E and the N directions, respectively. The settings of $\sigma_{a_{x,k}}$ and $\sigma_{a_{y,k}}$ reveal the dynamic behavior of non-abnormal vehicles moving on the road of which driving actions on the acceleration are along the x axis. Three dynamic models corresponding to the different accelerations of $0 m/s^2$, $-2 m/s^2$, $5 m/s^2$ are used, and the switching between any two of these three models is described by the first-order Markov chain φ with the transition probability $\pi_{pp}^\varphi = 0.8$ ($p = 1, 2, 3$), and $\pi_{pq}^\varphi = 0.1$ ($p \neq q$; $p, q = 1, 2, 3$). As shown in Fig. 1, the TV starts at the position (300, 10) in m , and then travels on the second lane from the West (W) to the East (E). The initial velocity is set as (90, 0) in km/h , and the TV starts to make an approximated uniform motion between 0 and 35 step, a slow-down movement with a deceleration of $-2 m/s^2$ between 36 and 40 step, a straight movement with a constant velocity between 41 and 65 step, a speed-up movement with an acceleration of $5 m/s^2$ between 66 and 70 step, and finally another uniform movement between 71 and 100 step.

It is assumed that the initial locations of all the neighbors are practically distributed within the road section according to the uniform distribution. The dynamics of the neighbors are subject to model (1). However, they keep a near stable

movement during the entire 100 steps. The DSRC communication range of each vehicle is set as 300 m, and only the neighbors under the DSRC coverage of the TV could beneficially contribute to the positioning enhancements for mobile vehicle localization. It is noted that a vehicle who holds that communication capability combined with the coarse measurements obtained from the GPS and the DSRC physical layer is defined as the vehicle who holds the CV technologies. The measurement process is represented by the model (9), and the measurement noise $\vartheta_k(\phi_k)$ is described by the Markov chain ϕ_k , which takes with the switching covariance matrix associated with the DFS and the RSSI measurements under the LOS and the NLOS conditions with the following formulations:

$$\mathbf{R}_k^{LOS} = \text{diag}(\sigma_{m_{x,k}}^{GPS^2}, \sigma_{m_{y,k}}^{GPS^2}, \sigma_{\dot{m}_{x,k}}^{GPS^2}, \sigma_{\dot{m}_{y,k}}^{GPS^2}, \sigma_{\rho_k^1}^{LOS,DFS^2}, \dots, \sigma_{\rho_k^i}^{LOS,DFS^2}, \sigma_{r_k^1}^{LOS,RSSI^2}, \dots, \sigma_{r_k^j}^{LOS,RSSI^2}), \quad (58)$$

and

$$\mathbf{R}_k^{NLOS} = \text{diag}(\sigma_{m_{x,k}}^{GPS^2}, \sigma_{m_{y,k}}^{GPS^2}, \sigma_{\dot{m}_{x,k}}^{GPS^2}, \sigma_{\dot{m}_{y,k}}^{GPS^2}, \sigma_{\rho_k^1}^{NLOS,DFS^2}, \dots, \sigma_{\rho_k^i}^{NLOS,DFS^2}, \sigma_{r_k^1}^{NLOS,RSSI^2}, \dots, \sigma_{r_k^j}^{NLOS,RSSI^2}), \quad (59)$$

respectively. For the GPS measurements, assume that the variance of the position and the velocity in the LOS and the NLOS conditions are fixed. In the 2-D localization problem the LOS and the NLOS conditions are used for depicting the different situation of the propagation channel on the DSRC signals that is paralleling to the road plane, whereas the propagation of the GPS signals is not in that plane, so as to take the variances of the GPS measurements as $\sigma_{m_{x,k}}^{GPS} = \sqrt{\frac{200}{2}} m$, $\sigma_{m_{y,k}}^{GPS} = \sqrt{\frac{200}{2}} m$, $\sigma_{\dot{m}_{x,k}}^{GPS} = \sqrt{\frac{15}{2}} m/s$, $\sigma_{\dot{m}_{y,k}}^{GPS} = \sqrt{\frac{15}{2}} m/s$, respectively. For the DFS measurements, the noise variance under the LOS condition is set as $\sigma_{\rho_k^1}^{LOS,DFS} = 100 Hz$, and that variance under the NLOS condition is set as $\sigma_{\rho_k^1}^{NLOS,DFS} = 120 Hz$. For the RSSI measurements, the transmission power related constant $C = 20$, and the path-loss exponent $\gamma = 3.5$. The noise variance under the

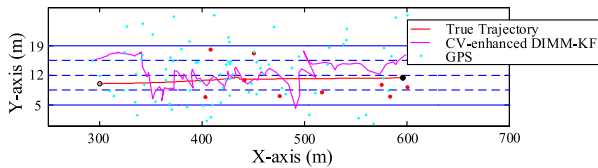


FIGURE 3. One trial demo of vehicular positioning estimation with both the DFS and the RSSI measurements.

LOS condition is set as $\sigma_{r_k}^{LOS,RSSI} = 5 \text{ dBm}$, and that variance under the NLOS condition is set as $\sigma_{r_k}^{NLOS,RSSI} = 30 \text{ dBm}$. The transition probability to describe the switching states between the LOS and the NLOS conditions is set as $\pi_{uu}^\phi = 0.9 (u = 1, 2)$, and $\pi_{uv}^\phi = 0.1 (u \neq v; u, v = 1, 2)$. Assume that the TV travels under the LOS condition at the beginning, entering into the NLOS condition between 30 and 80 step, and make a another transition into the LOS condition between 81 and 100 step.

B. SINGLE-TRIAL ANALYSIS

In order to verify the effectiveness of the proposed method, a single-trial test is used to clearly demonstrate the entire scenario in which the settings follow the parameters that are described in the Section IV-A. The true trajectory of the TV (i.e. the black circle and the black dot represent the initial and the ending positions of the TV, respectively), one trail of the estimated trajectory of the TV using the CV-enhanced DIMM-KF method, and the original GPS measurements of the TV are collectively shown in Fig. 3. Compared to the GPS-based positioning, the proposed CV-enhanced DIMM-KF method could provide much better performance on the vehicle localization throughout the entire process.

C. MONTE CARLO RESULTS

To evaluate the closeness from the estimated to the true trajectories, the RMSE metrics in position is deployed at each time step k . The definitions of the RMSE are formulated as (60), as shown at the bottom of this page, the root-mean-SPEB is $R.SPEB_k = \sqrt{\frac{1}{N_T} \sum_{T=1}^{N_T} SPEB_k(T)}$, and the root-mean-mSPEB is $R.mSPEB_k = \sqrt{\frac{1}{N_T} \sum_{T=1}^{N_T} mSPEB_k(T)}$.

In (60), $(\hat{m}_{x,k}(T), \hat{m}_{y,k}(T))$ denotes the estimated position vector in the T th Monte Carlo simulation. In Fig. 4, the comparison between the GPS-based positioning and the proposed CP method is conducted over $N_T = 1000$ Monte Carlo runs. Each of them follows the basic traffic settings that are described in the Section IV-A. Meanwhile, for the TV’s position, the R.SPEB and the R.mSPEB obtained from the FIM and the EFIM at each time step k are illustrated

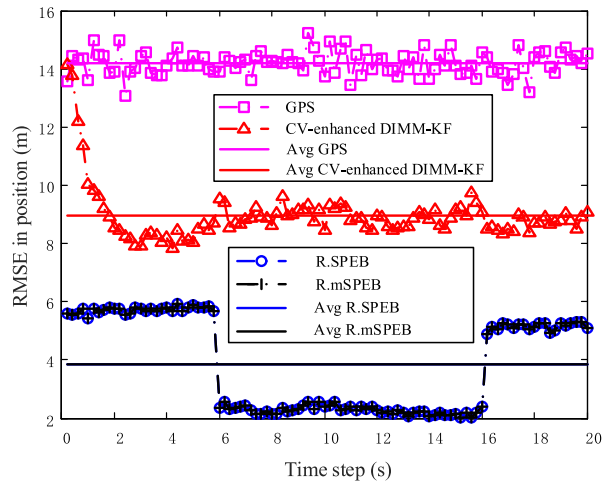


FIGURE 4. The performance of the GPS and the proposed method, and the fundamental limits bounded by the R.SPEB and the R.mSPEB.

as well. The results testify the achieved performance that is enhanced by the proposed CP method, and also indicate that the R.mSPEB is at least incredibly close to the R.SPEB in this specific 2-D case.

To analyze the enhanced performance of the proposed CP method on different traffic intensities and CV penetrations, the statistical simulations are created. Each case is imitated $N_T = 500$ times, and the average achievable performance for the combinations between the traffic intensity and the CV penetration was evaluated. Correspondingly, the traffic intensity is set ranging from 20 to 200 *vehicle/km*, and the CV penetration is set ranging from 25% to 100%. Both Fig. 5 and Fig. 6 are under consideration of the neighbors who can provide the DFS measurements to benefit the positioning performance on the TV. Fig. 5 shows that the enhancements on the vehicle localization system generally increases with the increase of the traffic intensity and the CV penetration, respectively. Additionally, in Fig. 6, it should be noted that a few outliers adversely affected the achieved performance when the traffic intensity is at a relative high level. Indeed, regardless of the traffic intensity, the number of the participated neighbors is a key factor to the CP method on the vehicle localization. Fig. 6 shows that the enhancement rate sternly increases with the increase of number of the participated neighbors. With regard to the performance metric defined as $\mu\% = \left[1 - \frac{RMSE_{CP}}{RMSE_{GPS}} \times 100\% \right]$, the enhancement rate over the GPS-based positioning reaches at about 35% to about 70%.

Both Fig. 7 and Fig. 8 are under consideration of the neighbors who can provide the RSSI measurements to benefit

$$RMSE_k = \sqrt{\frac{1}{N_T} \sum_{T=1}^{N_T} \left\{ (\hat{m}_{x,k}(T) - m_{x,k}(T))^2 + (\hat{m}_{y,k}(T) - m_{y,k}(T))^2 \right\}}, \tag{60}$$

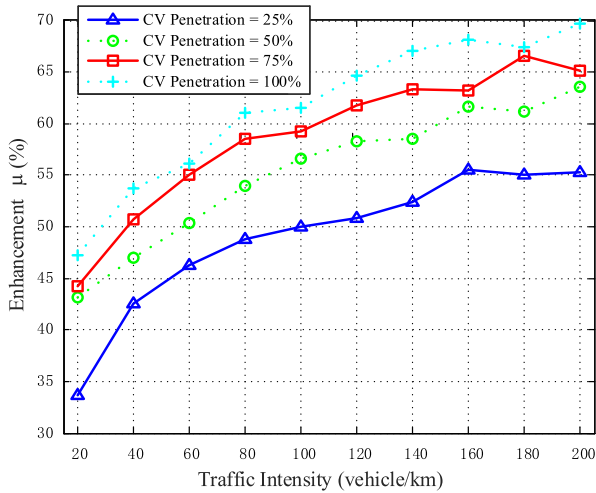


FIGURE 5. The enhancements for different CV penetrations - DFS only.

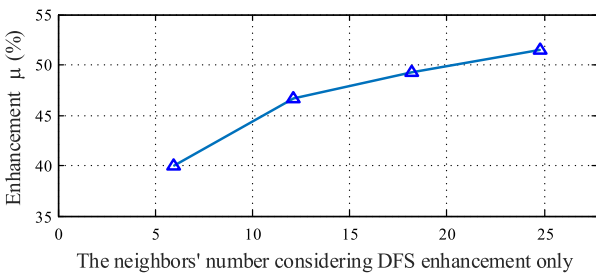


FIGURE 6. The neighbors' number and achieved performance - DFS only.

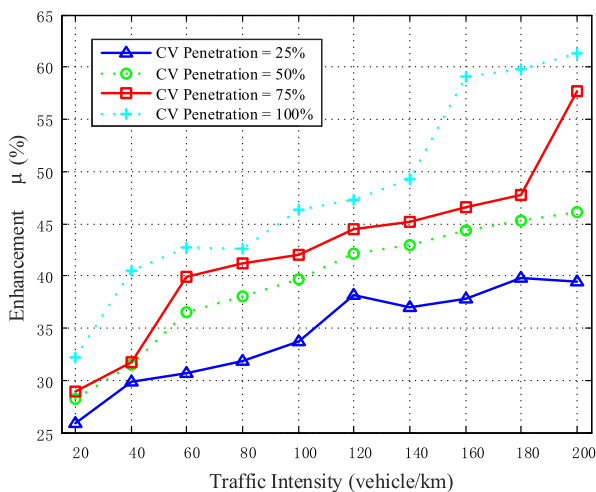


FIGURE 7. The enhancements for different CV penetrations - RSSI only.

the positioning performance on the TV. Fig. 7 and Fig. 8 show that the trend of the related increments is similar to Fig. 5 and Fig. 6, respectively. Correspondingly, the CV-enhancement method reaches at about 25% to about 60% over the GPS-based positioning.

Fig. 9 compares the CP method enhanced by using the DFS and the RSSI measurements with the other enhancement by only using the DFS measurements, showing that the proposed CP enhancement approach using more

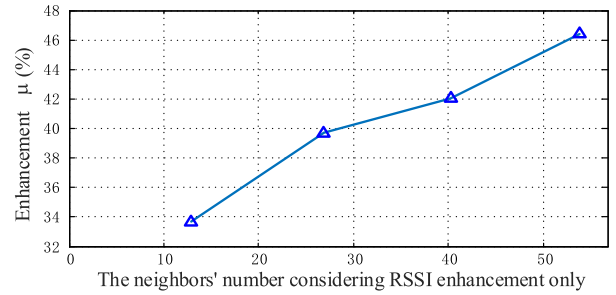


FIGURE 8. The neighbors' number and achieved performance - RSSI only.

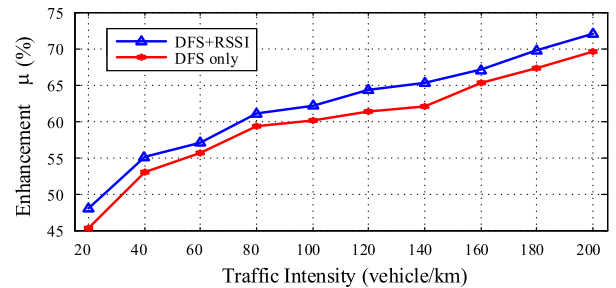


FIGURE 9. The enhancements for the DFS and the RSSI measurements combination, and for the DFS measurements only.

measurements' data can better improve the positioning performance for mobile vehicle localization. Significantly, the achieved enhancement rate is up to 72.10% when the traffic intensity is 50 vehicle/km/lane.

V. CONCLUSION

This paper proposed a novel method combined both the DFS and the RSSI measurements extracted from the DSRC physical layer to enhance the positioning accuracy for the vehicle localization system. Avoiding some range-based methods, the proposed CP method is designed to leverage both the range-rate (DFS) and the ranging (RSSI) measurements shared in the V2V communication environments. The feasibility and the performance of the method have been investigated through the following two types of simulations: 1) the single-trial analysis and 2) the Monte Carlo results. The achieved enhancement rate on the TV localization can be increased from about 35% to about 72% compared with the stand-alone GPS method, according to different traffic intensities and the CV penetrations. The proposed mSPEB is verified to bound the fundamental limits for localization systems with less computational complexity compared to the conventional SPEB. Additional insight that all inter-vehicle measurements can improve the CP estimation accuracy is provided from the point view of the CRLB.

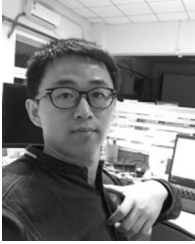
REFERENCES

- [1] N. Alam and A. G. Dempster, "Cooperative positioning for vehicular networks: Facts and future," *IEEE Trans. Intell. Transp. Syst.*, vol. 14, no. 4, pp. 1708–1717, Dec. 2013.
- [2] T. S. Rappaport, J. H. Reed, and B. D. Woerner, "Position location using wireless communications on highways of the future," *IEEE Commun. Mag.*, vol. 34, no. 10, pp. 33–41, Oct. 1996.

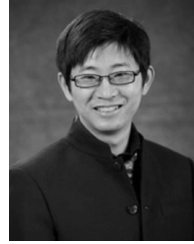
- [3] R. Zekavat and R. M. Buehrer, *Handbook of Position Location: Theory, Practice and Advances*, vol. 27. New York, NY, USA: Wiley, 2011.
- [4] S. E. Shladover and S.-K. Tan, "Analysis of vehicle positioning accuracy requirements for communication-based cooperative collision warning," *J. Intell. Transp. Syst.*, vol. 10, no. 3, pp. 131–140, 2006. [Online]. Available: <http://www.tandfonline.com/doi/abs/10.1080/15472450600793610>
- [5] R. Sengupta, S. Rezaei, S. E. Shladover, D. Cody, S. Dickey, and H. Krishnan, "Cooperative collision warning systems: Concept definition and experimental implementation," *J. Intell. Transp. Syst.*, vol. 11, no. 3, pp. 143–155, 2007. [Online]. Available: <http://www.tandfonline.com/doi/abs/10.1080/15472450701410452>
- [6] K. Zheng, Q. Zheng, P. Chatzimisios, W. Xiang, and Y. Zhou, "Heterogeneous vehicular networking: A survey on architecture, challenges, and solutions," *IEEE Commun. Surveys Tut.*, vol. 17, no. 4, pp. 2377–2396, 4th Quart. 2015.
- [7] Y.-C. Cheng, Y. Chawathe, A. LaMarca, and J. Krumm, "Accuracy characterization for metropolitan-scale Wi-Fi localization," in *Proc. 3rd Int. Conf. Mobile Syst., Appl. Serv.*, 2005, pp. 233–245.
- [8] S. Mazuelas et al., "Prior NLOS measurement correction for positioning in cellular wireless networks," *IEEE Trans. Veh. Technol.*, vol. 58, no. 5, pp. 2585–2591, Jun. 2009.
- [9] J. Wang, F. Adib, R. Knepper, D. Katabi, and D. Rus, "RF-compass: Robot object manipulation using RFIDs," in *Proc. 19th Annu. Int. Conf. Mobile Comput. Netw.*, 2013, pp. 3–14.
- [10] N. Alam, A. Kealy, and A. G. Dempster, "Cooperative inertial navigation for GNSS-challenged vehicular environments," *IEEE Trans. Intell. Transp. Syst.*, vol. 14, no. 3, pp. 1370–1379, Sep. 2013.
- [11] R. Yang, G. W. Ng, and Y. Bar-Shalom, "Tracking/fusion and deghosting with doppler frequency from two passive acoustic sensors," in *Proc. IEEE 16th Int. Conf. Inf. Fusion (FUSION)*, Jul. 2013, pp. 1784–1790.
- [12] M. Porretta, P. Nepa, G. Manara, and F. Giannetti, "Location, location, location," *IEEE Veh. Technol. Mag.*, vol. 3, no. 2, pp. 20–29, Jun. 2008.
- [13] Z. Yang, Z. Zhou, and Y. Liu, "From RSSI to CSI: Indoor localization via channel response," *ACM Comput. Surv. (CSUR)*, vol. 46, no. 2, 2013, Art. no. 25
- [14] N. Alam, A. T. Balaei, and A. G. Dempster, "A dsrc doppler-based cooperative positioning enhancement for vehicular networks with gps availability," *IEEE Trans. Veh. Technol.*, vol. 60, no. 9, pp. 4462–4470, Nov. 2011.
- [15] S. Coleri Ergen, H. S. Tetikol, M. Kontik, R. Sevlian, R. Rajagopal, and P. Varaiya, "RSSI-fingerprinting-based mobile phone localization with route constraints," *IEEE Trans. Veh. Technol.*, vol. 63, no. 1, pp. 423–428, Jan. 2014.
- [16] M. Chen, Y. Zhang, L. Hu, T. Taleb, and Z. Sheng, "Cloud-based wireless network: Virtualized, reconfigurable, smart wireless network to enable 5G technologies," *Mobile Netw. Appl.*, vol. 20, no. 6, pp. 704–712, Dec. 2015.
- [17] H. Aly, A. Basalamah, and M. Youssef, "Lanequest: An accurate and energy-efficient lane detection system," in *Proc. IEEE Int. Conf. Pervas. Comput. Commun. (PerCom)*, 2015, pp. 163–171.
- [18] N. Alam, A. T. Balaei, and A. G. Dempster, "An instantaneous lane-level positioning using DSRC carrier frequency offset," *IEEE Trans. Intell. Transp. Syst.*, vol. 13, no. 4, pp. 1566–1575, Dec. 2012.
- [19] Y. Zhang, M. Chen, S. Mao, L. Hu, and V. Leung, "CAP: Community activity prediction based on big data analysis," *IEEE Netw.*, vol. 28, no. 4, pp. 52–57, Jul./Aug. 2014.
- [20] Y. Zhang, "GroRec: A group-centric intelligent recommender system integrating social, mobile and big data technologies," *IEEE Trans. Serv. Comput.*, vol. 9, no. 5, pp. 786–795, May 2016.
- [21] M. Chen, Y. Ma, J. Song, C.-F. Lai, and B. Hu, "Smart clothing: Connecting human with clouds and big data for sustainable health monitoring," *Mobile Netw. Appl.*, vol. 21, no. 5, pp. 825–845, 2016. [Online]. Available: <http://dx.doi.org/10.1007/s11036-016-0745-1>
- [22] G. Sun, J. Chen, W. Guo, and K. J. R. Liu, "Signal processing techniques in network-aided positioning: A survey of state-of-the-art positioning designs," *IEEE Signal Process. Mag.*, vol. 22, no. 4, pp. 12–23, Jul. 2005.
- [23] A. H. Sayed, A. Tarighat, and N. Khajehnouri, "Network-based wireless location: Challenges faced in developing techniques for accurate wireless location information," *IEEE Signal Process. Mag.*, vol. 22, no. 4, pp. 24–40, Jul. 2005.
- [24] M. Z. Win et al., "Network localization and navigation via cooperation," *IEEE Commun. Mag.*, vol. 49, no. 5, pp. 56–62, May 2011.
- [25] T. S. Dao, K. Y. K. Leung, C. M. Clark, and J. P. Huissoon, "Markov-based lane positioning using intervehicle communication," *IEEE Trans. Intell. Transp. Syst.*, vol. 8, no. 4, pp. 641–650, Dec. 2007.
- [26] Y. Wang, X. Duan, D. Tian, G. Lu, and H. Yu, "Throughput and delay limits of 802.11p and its influence on highway capacity," *Proc.-Social Behavioral Sci.*, vol. 96, pp. 2096–2104, Nov. 2013. [Online]. Available: <http://www.sciencedirect.com/science/article/pii/S1877042813023628>
- [27] Y. Shen, S. Mazuelas, and M. Z. Win, "Network navigation: Theory and interpretation," *IEEE J. Sel. Areas Commun.*, vol. 30, no. 9, pp. 1823–1834, Oct. 2012.
- [28] K. Zheng, H. Meng, P. Chatzimisios, L. Lei, and X. Shen, "An SMDP-based resource allocation in vehicular cloud computing systems," *IEEE Trans. Ind. Electron.*, vol. 62, no. 12, pp. 7920–7928, Dec. 2015.
- [29] J. M. Huerta, J. Vidal, A. Giremus, and J.-Y. Tourneret, "Joint particle filter and UKF position tracking in severe non-line-of-sight situations," *IEEE J. Sel. Topics Signal Process.*, vol. 3, no. 5, pp. 874–888, Oct. 2009.
- [30] N. Alam, A. T. Balaei, and A. G. Dempster, "Relative positioning enhancement in VANETS: A tight integration approach," *IEEE Trans. Intell. Transp. Syst.*, vol. 14, no. 1, pp. 47–55, Mar. 2013.
- [31] X. R. Li and V. P. Jilkov, "Survey of maneuvering target tracking. Part I. Dynamic models," *IEEE Trans. Aerosp. Electron. Syst.*, vol. 39, no. 4, pp. 1333–1364, Oct. 2003.
- [32] W. Li and Y. Jia, "Location of mobile station with maneuvers using an IMM-based cubature Kalman filter," *IEEE Trans. Ind. Electron.*, vol. 59, no. 11, pp. 4338–4348, Nov. 2012.
- [33] Y. Chang-Yi, B.-S. Chen, and L. Feng-Ko, "Mobile location estimation using fuzzy-based imm and data fusion," *IEEE Trans. Mobile Comput.*, vol. 9, no. 10, pp. 1424–1436, Oct. 2010.
- [34] B. S. Chen, C. Y. Yang, F. K. Liao, and J. F. Liao, "Mobile location estimation in a rough wireless environment using extended Kalman-based IMM and data fusion," *IEEE Trans. Veh. Technol.*, vol. 58, no. 3, pp. 1157–1169, Mar. 2009.
- [35] T. S. Rappaport, *Wireless Communications: Principles and Practice*, vol. 2. Englewood Cliffs, NJ, USA: Prentice-Hall, 1996.
- [36] W. Viriyasitavat, M. Boban, H. M. Tsai, and A. Vasilakos, "Vehicular communications: Survey and challenges of channel and propagation models," *IEEE Veh. Technol. Mag.*, vol. 10, no. 2, pp. 55–66, Jun. 2015.
- [37] W. Li, Y. Jia, J. Du, and J. Zhang, "Distributed multiple-model estimation for simultaneous localization and tracking with NLOS mitigation," *IEEE Trans. Veh. Technol.*, vol. 62, no. 6, pp. 2824–2830, Jul. 2013.
- [38] W. Li and Y. Jia, "Consensus-based distributed multiple model UKF for jump Markov nonlinear systems," *IEEE Trans. Autom. Control*, vol. 57, no. 1, pp. 227–233, Jan. 2012.
- [39] S. Yuan and M. Z. Win, "Fundamental limits of wideband localization—Part I: A general framework," *IEEE Trans. Inf. Theory*, vol. 56, no. 10, pp. 4956–4980, Oct. 2010.
- [40] J. Prieto, S. Mazuelas, A. Bahillo, P. Fernandez, R. M. Lorenzo, and E. J. Abril, "Adaptive data fusion for wireless localization in harsh environments," *IEEE Trans. Signal Process.*, vol. 60, no. 4, pp. 1585–1596, Apr. 2012.
- [41] H. L. Van Trees, *Detection, Estimation, and Modulation Theory*. New York, NY, USA: Wiley, 2004.
- [42] R. A. Horn and C. R. Johnson, *Matrix Analysis*. Cambridge, U.K.: Cambridge Univ. Press, 1986.
- [43] Z. Bai and G. H. Golub, "Bounds for the trace of the inverse and the determinant of symmetric positive definite matrices," *Ann. Numer. Math.*, vol. 4, pp. 29–38, Apr. 1996.
- [44] P. D. Robinson and A. J. Wathen, "Variational bounds on the entries of the inverse of a matrix," *IMA J. Numer. Anal.*, vol. 12, no. 4, pp. 463–486, 1992. [Online]. Available: <http://imajna.oxfordjournals.org/content/12/4/463.abstract>



YUNPENG WANG is currently a Professor with the School of Transportation Science and Engineering, Beihang University, Beijing, China. His current research interests include intelligent transportation systems, traffic safety, and vehicle infrastructure integration.



XUTING DUAN is currently pursuing the Ph.D. degree with the School of Transportation Science and Engineering, Beihang University, Beijing, China. His current research focuses on vehicle-to-anything communication systems, cooperative positioning, and localization network optimization.



MIN CHEN is currently a Professor with the School of Computer Science and Technology, Huazhong University of Science and Technology, Wuhan, China. His research interests include cyber physical systems, Internet of Things sensing, 5G networks, mobile cloud computing, SDN, healthcare big data, medical cloud privacy and security, body area networks, emotion communications, and robotics.



DAXIN TIAN is currently an Associate Professor with the School of Transportation Science and Engineering, Beihang University, Beijing, China. His current research interests include mobile computing, intelligent transportation systems, vehicular ad hoc networks, and swarm intelligent.



XUEJUN ZHANG received the B.S. and Ph.D. degrees from Beihang University in 1994 and 2000, respectively. He is currently a Professor with the School of Electronic and Information Engineering, Beihang University. He is also the Deputy Director of the National Key Laboratory of CNS/ATM, China. His main research interests are air traffic management, data communication, and air surveillance.

...